香港天文台
HONG KONG OBSERVATORY

Reprint 1276

Projection of wet-bulb temperature for Hong Kong in the 21st century using CMIP5 data

Hang-wai TONG, Chau-ping WONG & Sai-ming LEE

利用 CMIP5 數據推算香港 21 世紀濕球溫度

唐恒偉　　　黃秋平　　　李細明
香港天文台

摘要

在全球暖化的背景下，一般預料暑熱壓力會升高，人體舒適度會下降，引起公眾關注氣候暖化對人類健康的影響。濕球溫度與濕潤表面的散熱程度有關，是一個暑熱壓力的基本指標。高濕球溫度表示環境既暖又濕，散熱較困難。本文利用政府間氣候變化專門委員會第五份評估報告中的 CMIP5 模式逐日數據進行降尺度統計分析，以推算 21 世紀香港每年最高濕球溫度的趨勢和每年極端「暖濕」日數的變化，並探討在不同溫室氣體濃度情景下香港「暖濕」季節長度的變化。

Projection of wet-bulb temperature for Hong Kong in the 21st century using CMIP5 data

TONG Hang-wai　　WONG Chau-ping　　LEE Sai-ming
Hong Kong Observatory

Abstract

Against the background of global warming, it is generally expected that heat stress would increase and thermal comfort would decrease, raising concerns about the impact of a warming climate on human health. A basic indicator of heat stress is the wet-bulb temperature which is related to the heat loss over a damp surface. High wet-bulb temperatures indicate a warm and humid environment in which heat loss would be suppressed. In this study, CMIP5 model daily data used in the IPCC Fifth Assessment Report were statistically downscaled to project the trends of annual maximum wet-bulb temperature and the change in the annual number of extremely warm-and-humid days for Hong Kong in the 21st century. Changes in the duration of the warm-and-humid season in Hong Kong under various greenhouse gas concentration scenarios were examined.

1. Introduction

Against the backdrop of climate change, temperature is expected to rise further in this century. Meanwhile, the ability of the atmosphere to hold moisture will also be enhanced in conjunction with the temperature rise. Under high temperature and high humidity environment, the evaporative cooling effect of sweating may be reduced, and hence heat stress becomes a significant concern under the impact of climate change.

Wet-bulb temperature is a measure of both temperature and humidity, and therefore is a suitable index in investigating the impact of climate change on heat stress. While the core temperature of human body is around 37°C, the skin temperature is slightly cooler at 35°C. If the environmental wet-bulb temperature exceeds 35°C, then human body would be unable to dissipate heat by sweating, leading to hyperthermia. As such, 35°C is often taken to be a threshold to gauge human adaptability [1, 2].

In this study, CMIP5 model daily data under the four greenhouse gas concentration scenarios, i.e. RCP2.6 (low), RCP4.5 (medium-low), RCP6.0 (medium-high), RCP8.5 (high), are statistically downscaled to project the changes in wet-bulb temperature in Hong Kong for the 21st century. Section 2 presents the data used in this study including observations, re-analysis data and CMIP5 model data; Section 3 describes the statistical downscaling methodology; results are presented in Section 4, followed by concluding remarks in Section 5.

2. Data

2.1 Observation and re-analysis

Historical daily maximum wet-bulb temperature ($T_w$max) recorded at the Hong Kong Observatory (HKO) during 1966-2005 are used for training and verification purposes in the statistical downscaling process. Near-surface and upper-air parameters of the NCEP 20th Century Re-analysis Version 2 (20CR, [3]) averaged over southern China and the northern part of the South China Sea (108-120°E, 16-30°N) are examined as large-scale predictors in constructing the statistical downscaling model. The NCEP 20CR data have a horizontal resolution of 2 x 2 degrees.

2.2 CMIP5 model data

Daily data of a number of CMIP5 models (Table 1) with different horizontal resolution are acquired from the Program for Climate Model Diagnosis and Intercomparison website (http://pcmdi9.llnl.gov). There are 23 models offering projections (2006-2100) under the RCP4.5 and RCP8.5 scenarios, but only 13 and 11 models for the RCP2.6 and RCP6.0 scenarios respectively. Historical simulations of the CMIP5 models during the period 1966-2005 are used to evaluate the statistical downscaling model while future simulations under the four scenarios are used to generate projections for Hong Kong. To match the horizontal resolution of NCEP 20CR data, CMIP5 model data are re-gridded using bi-linear interpolation to a resolution of 2 x 2 degrees.

3.   Methodology

3.1   Statistical downscaling

Global climate models used for climate studies and climate projections are usually run at a coarse spatial resolution, which are inadequate to represent sub-grid scale features.   There are two downscaling approaches: dynamical downscaling and statistical downscaling. Dynamical downscaling involves the use of a regional climate model and is computationally demanding.   Here, we adopt the statistically downscaling approach because it has skill comparable with dynamical downscaling while computationally more economical.

3.2 Predictor selection

Wet-bulb temperature is related to near-surface temperature and humidity.   However, Huth (2005) [4] found that surface humidity variables were most accurately downscaled from the same variables at 850 hPa.   Hence specific humidity and relative humidity at 850 hPa instead of 1000 hPa are considered in the downscaling process in this study, and two predictor sets are used for the statistical model:

Set 1: 1000 hPa daily maximum temperature, 850 hPa specific humidity
Set 2: 1000 hPa daily maximum temperature, 850 hPa relative humidity

3.3 Standardization

To reduce systematic biases, it is a common practice to standardize the predictors and predictands in building and applying the statistical downscaling model [5].   Here, 1966-2005 is taken as the reference period for standardization.   The standardized predictors and predictands are then used to construct the statistical model.   Outcomes of the statistical model will be adjusted for variance while preserving the long-term trend, followed by de-standardization.

3.4 Multiple linear regression

Multiple linear regression is invoked with the standardized $T_w$max as the predictand.   A regression relationship between the predictand and the standardized predictors is established for each month.   The workflow is illustrated in Figure 1.   Normally, the variance of regression outcomes is smaller than that of the observations and variance adjustment is needed.   Here we adopt the variance inflation method in which the regression outcomes will be multiplied by the factor:

$$\frac{\text{standard deviation of observations}}{\text{standard deviation of regression outcomes}}$$

where the standard deviations are computed over the same reference period (1966-2005). To preserve the long-term trend of the regression results, the following procedures are adopted:

(a)   the regression outcomes are first de-trended by simple linear regression;
(b)   variance inflation is applied to the de-trended outcomes from (a); and
(c)   the linear trend obtained in (a) is then added back to the inflated outcomes from (b).

4. Results

4.1 Validation of the statistical model

Validation and projection results are based on the grand ensemble mean of projections using the two predictor sets (Section 3.2). Uncertainties of the projections are assessed through the spread of the ensemble, viz the 5th and 95th percentile of the grand ensemble. This spread is considered as the "likely range" of the projections, following the convention used in the IPCC Fifth Assessment Report [6].

The cross validation approach is employed to evaluate the statistical model. A block of observed $T_w$max of five years is omitted in turn, i.e. 1966-1970, 1971-1975, 1976-1980, 1981-1985, 1986-1990, 1991-1995, 1996-2000, 2001-2005. Regression equations are constructed using the remaining data. The equations are then used to generate predictions for the omitted days, using NCEP 20CR data as predictors.

We examine the performance of the statistical model for April-September, and Figure 2 shows the scatter plot of predicted and observed monthly average $T_w$max during the period. The correlation between the predictions and observations is 0.96, which is statistically significant.

4.2 Performance in simulating the past climate

It is also essential to evaluate the performance of the statistical model using CMIP5 model data rather than re-analysis data as predictors. The performance of the statistical downscaling model is found to be satisfactory. The $T_w$max averaged over April-September 1966-2005 is 25.5°C for both observation and downscaled prediction (Table 2). We define extremely warm-and-humid day (XWHD) as days with $T_w$max at or above the 99th percentile of the observed $T_w$max during 1966-2005. Table 2 shows that the downscaling result of annual number of XWHD averaged over 1966-2005 is higher than, but within one standard deviation of, the observation.

4.3 Projection for the 21st century

We investigate how the risk of high heat stress would change in the future by examining the projections of XWHD under different RCP scenarios. Results show that the annual number of XWHD is expected to increase regardless of the scenarios (Figure 3). Results also show that the maximum number of consecutive XWHD is expected to increase as well, suggesting that the duration of high heat stress will increase in the 21st century (Figure 4). The annual maximum of $T_w$max (TWXX) can be considered as indicative of the severity of heat stress, and Figure 5 shows that TWXX could exceed 31°C under the RCP8.5 scenario. Even for the RCP4.5 and RCP6.0 scenarios, TWXX could exceed 30°C in the latter part of this century. Sherwood and Huber (2010) [1] showed that $T_w$max on Earth never exceeded 31°C during 1999-2008. A situation of $T_w$max exceeding 30°C is therefore comparable to the most extreme heat stress experienced on Earth in recent times.

The duration of warm-and-humid season is also investigated. Hong Kong has a warm and humid summer and a cool and dry winter. Here we define warm-and-humid day as days with $T_w$max at or above the 75th percentile of the observed $T_w$max during 1966-2005.

According to this definition, warm-and-humid days start to emerge around mid-June and retreat around early September (Figure 6), which is roughly consistent with the onset and retreat of southwesterlies in Hong Kong.   Figure 7 shows that warm-and-humid days would occur as early as late April and extend well into October under the RCP8.5 scenario.   To a lesser extent, the trends of a prolonged warm-and-humid season under a warming climate are similarly observed under the RCP2.6, RCP4.5 and RCP6.0 scenarios.

5.   Concluding remarks

Daily data of CMIP5 models under different greenhouse gas concentration scenarios are statistically downscaled to project the changes in $T_w$max in Hong Kong in the 21st century. Projection results indicate that even under the RCP4.5 and RCP6.0 scenarios, the duration of high heat stress as well as the severity of heat stress would increase.   The warm-and-humid season in Hong Kong will also be extended.

The projection results suggest that there might be significant implications on the human comfort and public health aspects in a densely populated city like Hong Kong.   Unless there are intelligent and environment-friendly adaptation measures in the planning of future cities to mitigate such impacts, the outdoor urban environment will only get even hotter and more stressful as a result of the popular reaction of using more air-conditioning to solve the problem, and the consumption of more electricity and power to achieve that will only exacerbate the greenhouse gas emission scenarios in the absence of alternative and affordable clean energy.

References

[1] Sherwood, S. C. and M. Huber, 2010: An adaptability limit to climate change due to heat stress. *Proc. Natl Acad. Sci.*, **107**, 9552-9555.

[2] Pal, J. S and E. A. B. Eltahir, 2016: Future temperature in southwest Asia projected to exceed a threshold for human adaptability. *Nat. Clim. Change*, **6**, 197-200.

[3] Compo and Coauthors, 2011: The twentieth century reanalysis project. *Q. J. R. Meteorol. Soc.*, **137**, 1-28.

[4] Huth, R., 2005: Downscaling of humidity variables: a search for suitable predictors and predictands. *Int. J. Climatol.*, **25**, 243-250.

[5] Wilby, R.L., S. P. Charles, E. Zorita, B. Timbal, P. Whetton, L. O. Mearns, 2004: The guidelines for use of climate scenarios developed from statistical downscaling methods. Supporting material of the Intergovernmental Panel on Climate Change (IPCC), prepared on behalf of Task Group on Data and Scenario Support for Impacts and Climate Analysis (TGICA).

[6] IPCC, 2013: Long-term Climate Change: Projections, Commitments and Irreversibility. In: Climate Change 2013: The Physical Science Basis. Contribution of Working Group I to the Fifth Assessment Report of the Intergovernmental Panel on Climate Change [Stocker, T.F., D. Qin, G.-K. Plattner, M. Tignor, S.K. Allen, J. Boschung, A. Nauels, Y. Xia, V. Bex and P.M. Midgley (eds.)]. Cambridge University Press, Cambridge, United Kingdom and New York, NY, USA.

Table 1   Global climate models used in this study

Model	Center	RCP4.5	RCP8.5	RCP2.6	RCP6.0
ACCESS1-0	CSIRO	✓	✓		
BCC-CSM1-1	BCC	✓	✓	✓	✓
BNU-ESM	BNU	✓	✓	✓	
CanESM2	CCCma	✓	✓	✓	
CNRM-CM5	CNRM	✓	✓	✓	
CSIRO-Mk3-6-0	CSIRO	✓	✓	✓	✓
GFDL-ESM2G	NOAA GFDL	✓	✓		✓
GFDL-ESM2M	NOAA GFDL	✓	✓		✓
HadGEM2-CC	UKMO Had	✓	✓		
IPSL-CM5A-LR	IPSL	✓	✓	✓	✓
IPSL-CM5A-MR	IPSL	✓	✓	✓	✓
IPSL-CM5B-LR	IPSL	✓	✓		
MIROC5	MIROC	✓	✓	✓	✓
MIROC-ESM	MIROC	✓	✓		
MIROC-ESM-CHEM	MIROC	✓	✓	✓	✓
MPI-ESM-LR	MPI	✓	✓	✓	
MRI-CGCM	MRI	✓	✓		✓
Nor-ESM1-M	NCC	✓	✓	✓	✓
MPI-ESM-MR	MPI	✓	✓	✓	
ACCESS1-3	CSIRO	✓	✓		
BCC-CSM1-1-m	BCC	✓	✓	✓	✓
CMCC-CMS	CMCC	✓	✓		
CMCC-CM	CMCC	✓	✓		

Table 2   Statistical downscaling results for T_wmax averaged over April-September 1966-2005 and annual number of XWHD averaged over 1966-2005

|	TWmax (averaged over April-September)	Annual number of XWHD
Downscaling result	25.5°C	6.2 days
Observation	25.5°C	3.9 days
Standard deviation of observation	0.3°C	3.8 days
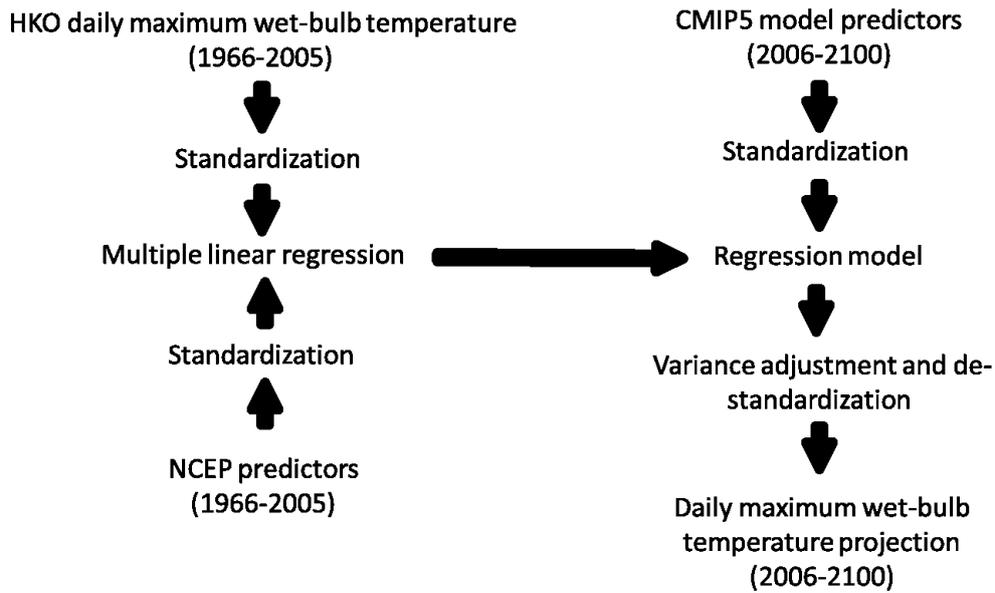
**Figure 1** Workflow of the statistical downscaling model.
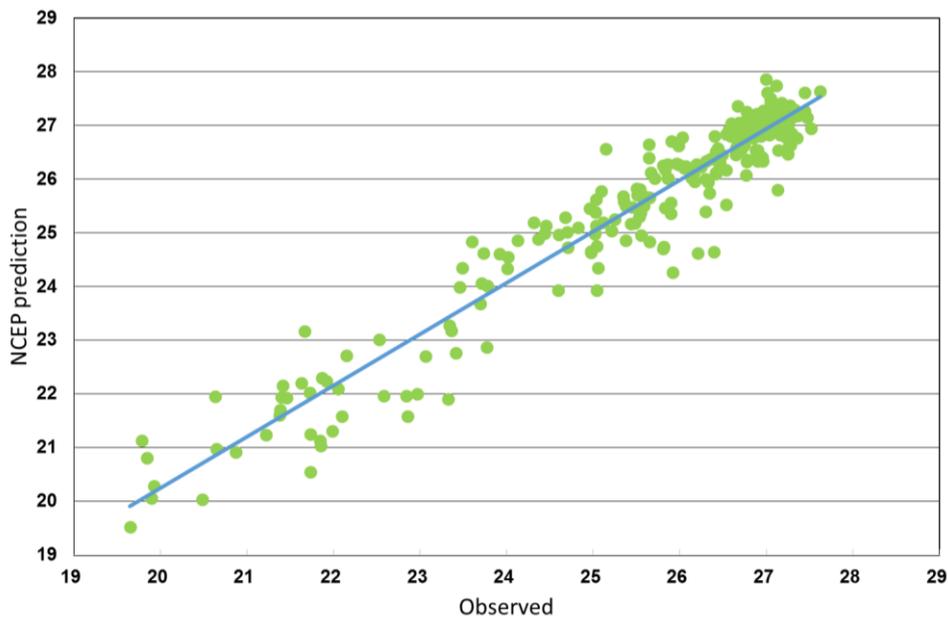
Figure 2 Predicted (using the cross-validation approach) and observed monthly average $T_w$max from April to September in 1966-2005.
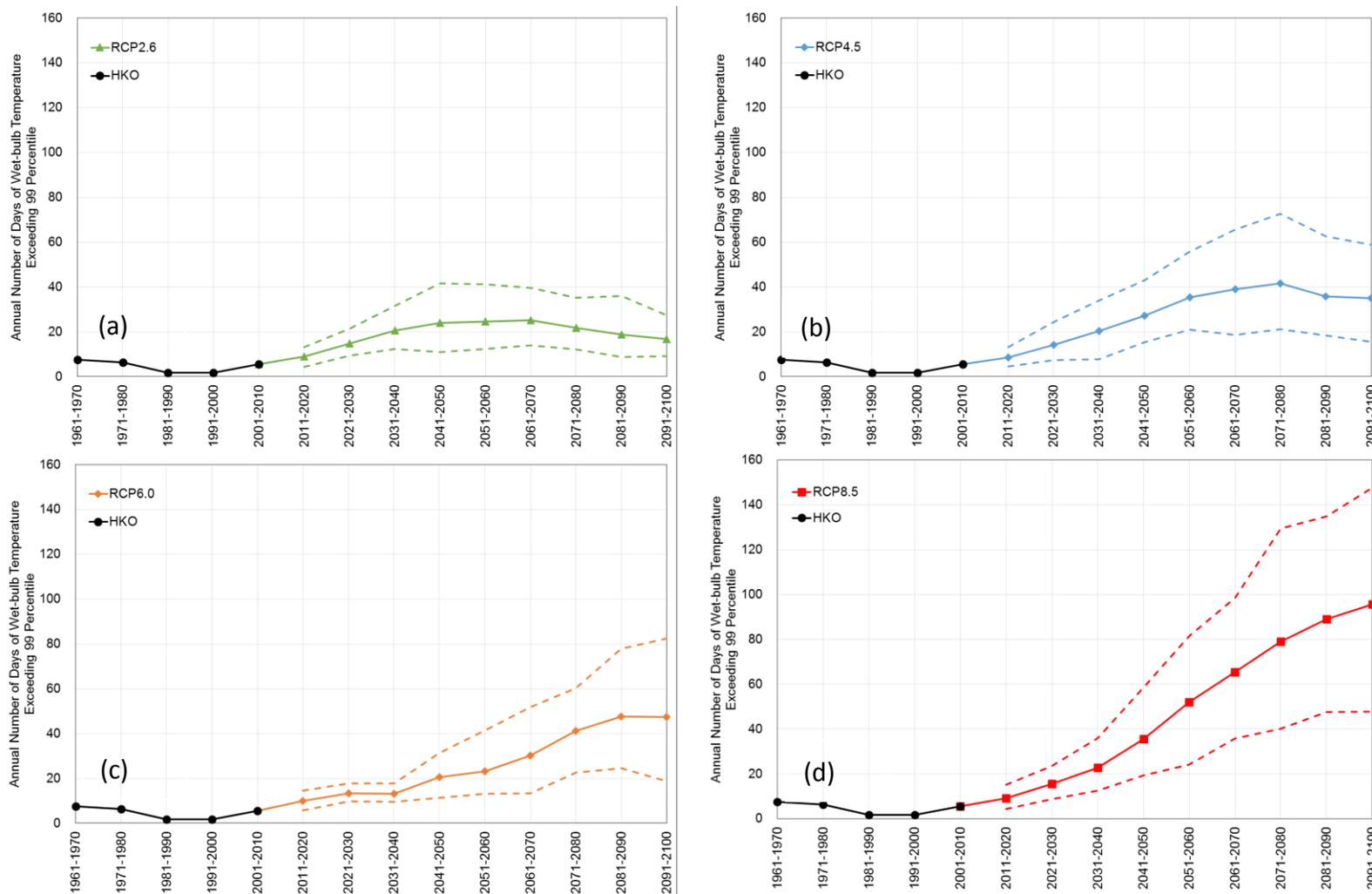
Figure 3 Projected decadal average of annual number of XWHD under: (a) RCP2.6, (b) RCP4.5, (c) RCP6.0 and (d) RCP8.5. Black line plots the observed value at Hong Kong Observatory. Solid coloured line plots the mean value and dashed coloured lines show the likely range of projection results.
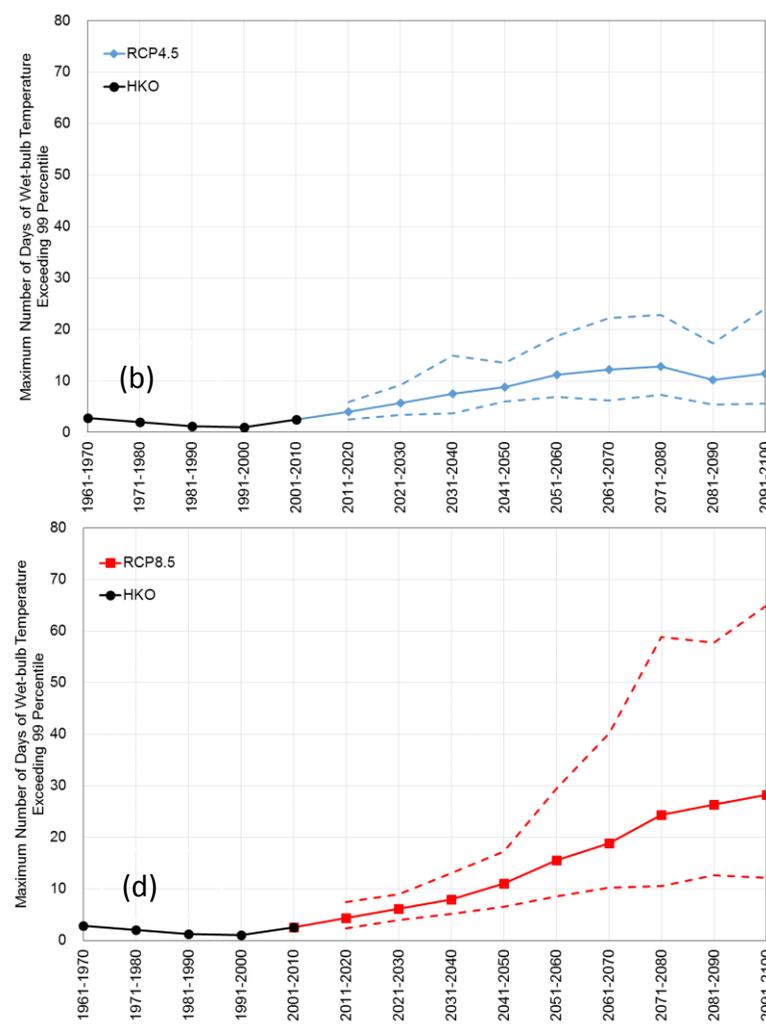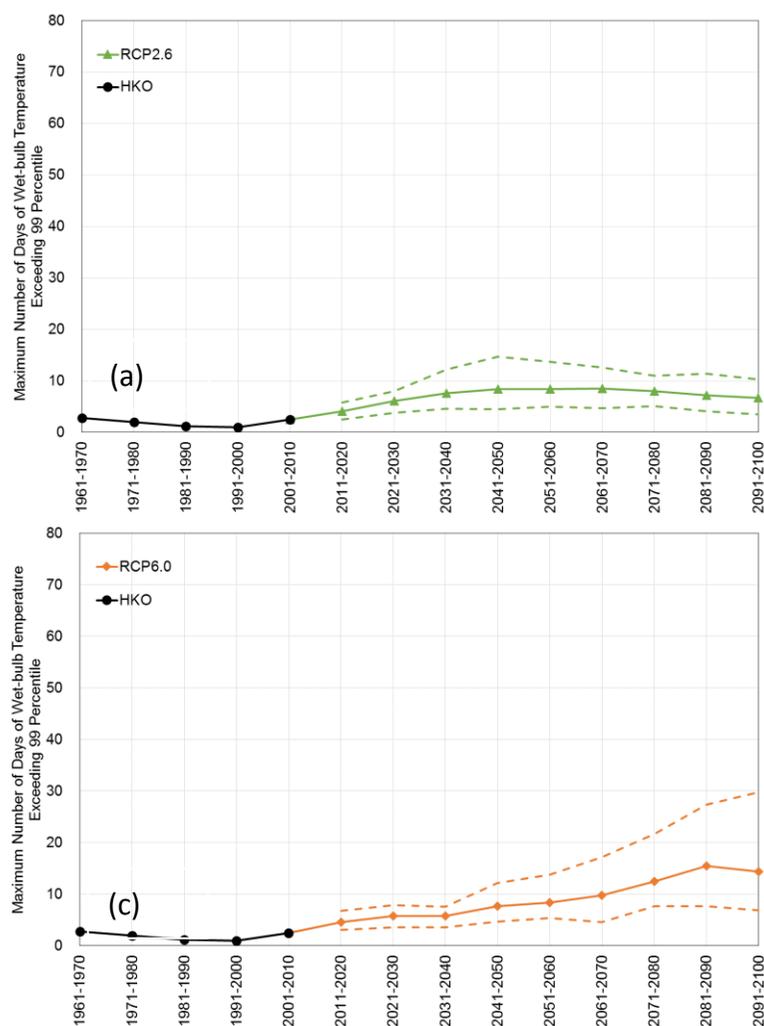
Figure 4 Projected decadal average of annual maximum number of consecutive XWHD under: (a) RCP2.6, (b) RCP4.5, (c) RCP6.0 and (d) RCP8.5. Black line plots the observed value at Hong Kong Observatory. Solid coloured line plots the mean value and dashed coloured lines show the likely range of projection results.
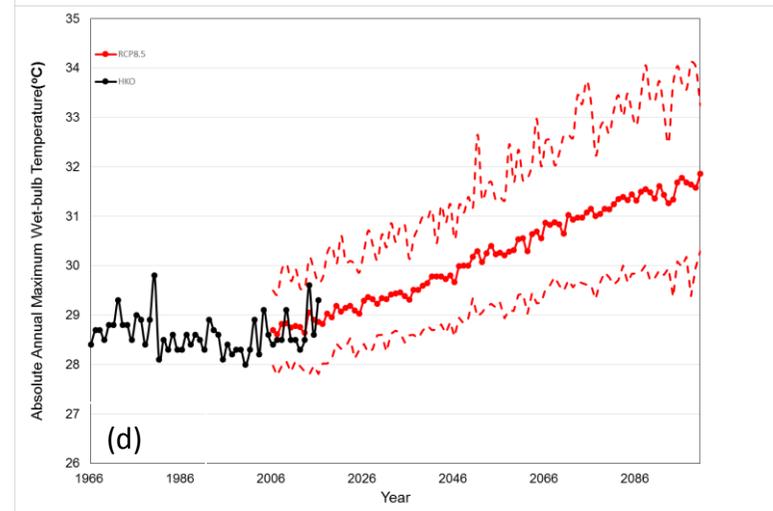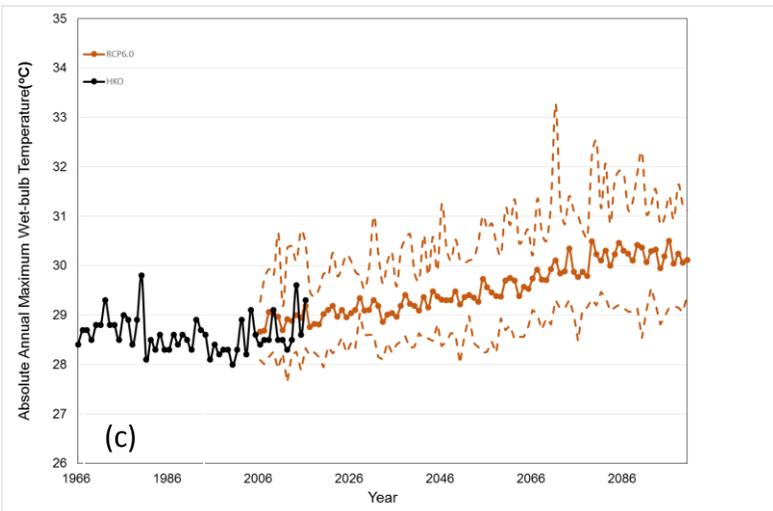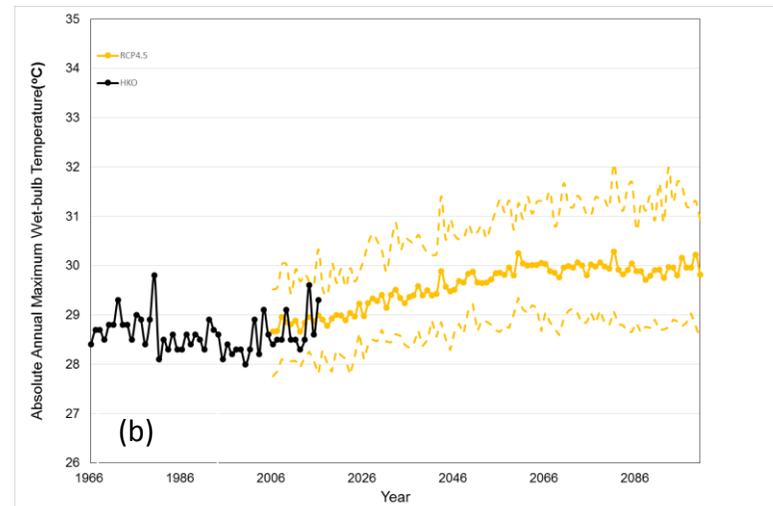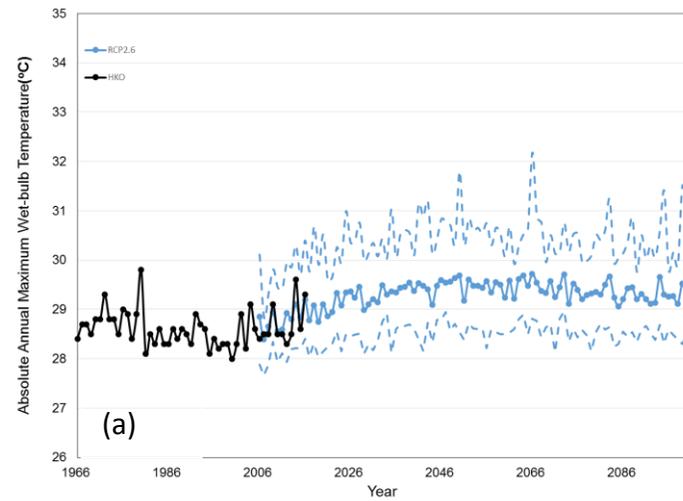
Figure 5   Projected changes in TWXX under: (a) RCP2.6, (b) RCP4.5, (c) RCP6.0 and (d) RCP8.5. Black line plots the observed value at Hong Kong Observatory. Solid coloured line plots the mean value and dashed coloured lines show the likely range of projection results.
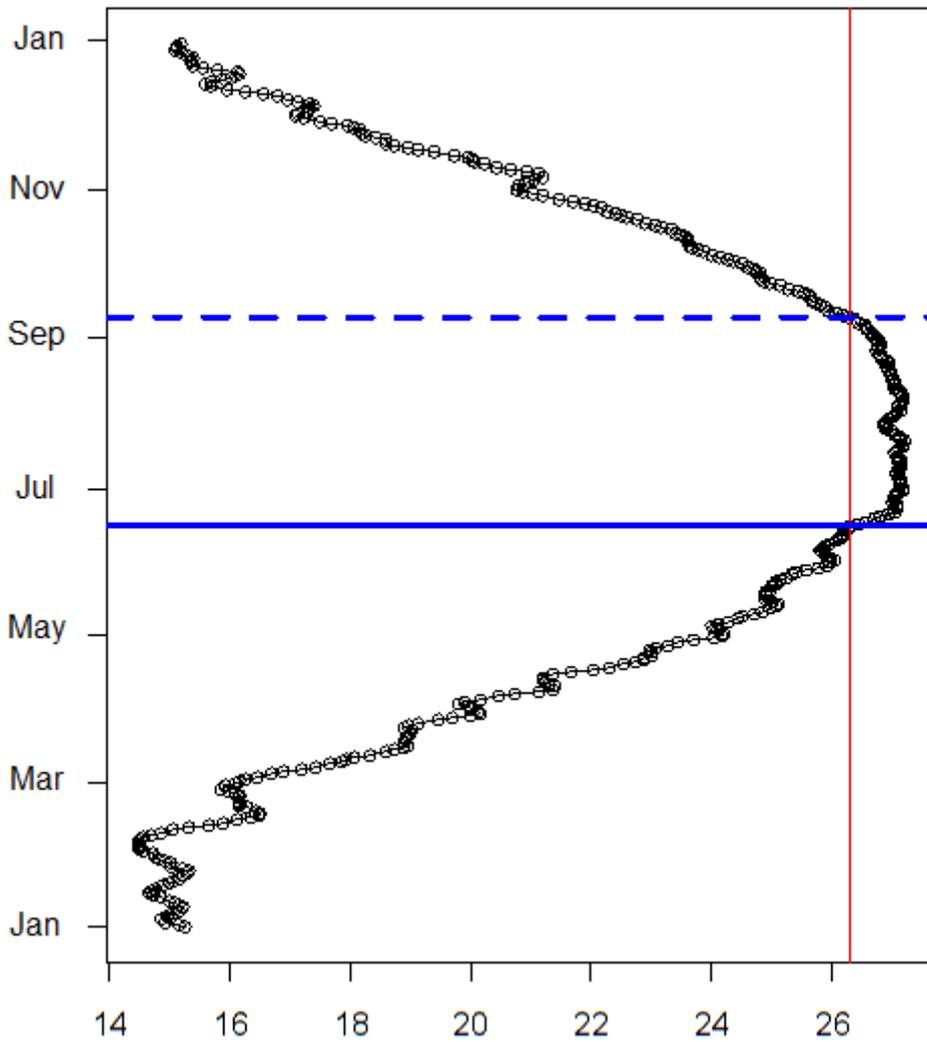
Figure 6 Climatological $T_w$max during 1966-2005. The red solid line denotes the 75th percentile of the observed values during 1966-2005. The solid and dashed blue lines denote the start and end of the warm-and-humid season respectively.
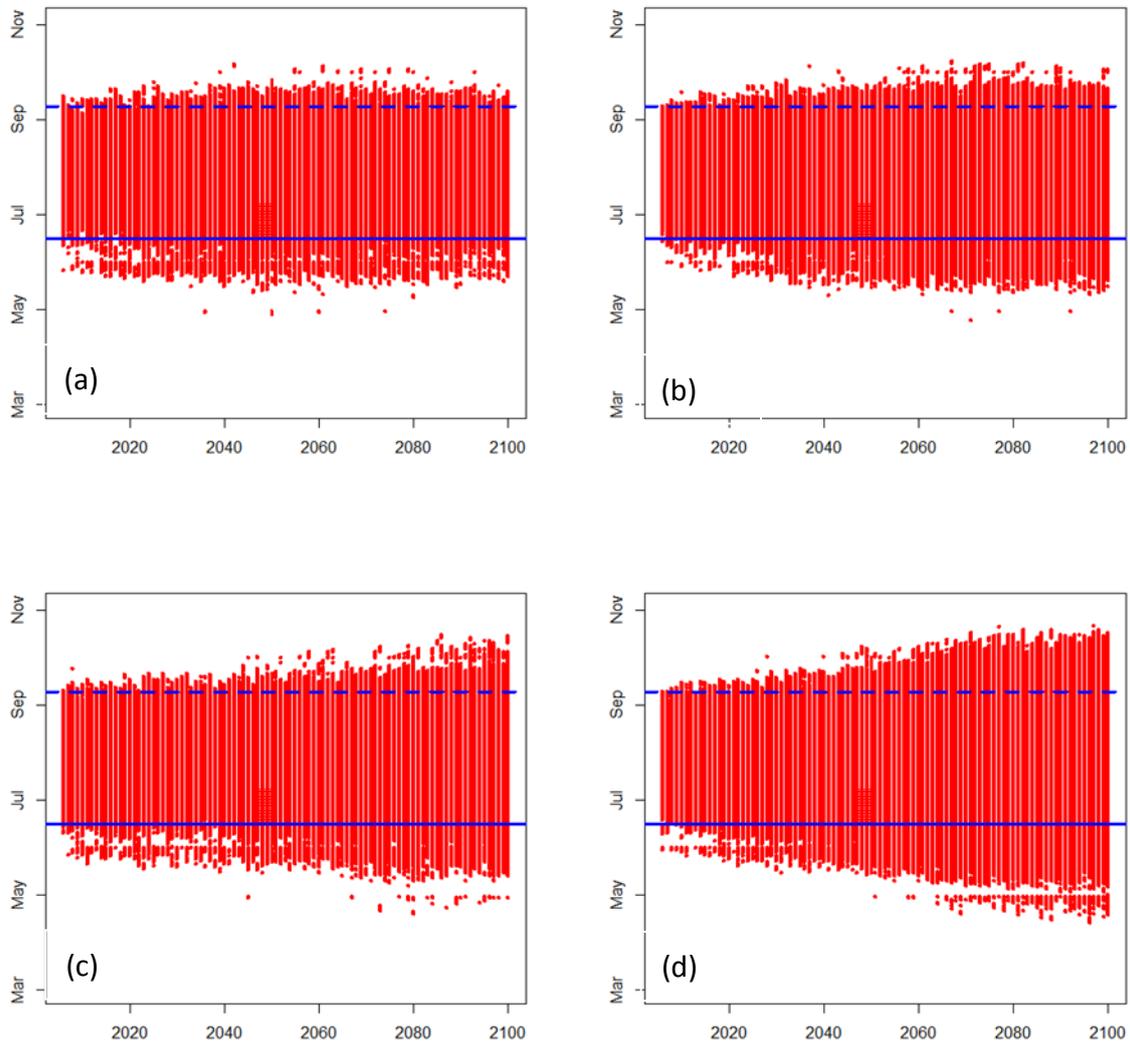
Figure 7 Projected changes in warm–and-humid days in the 21st century under: (a) RCP2.6, (b) RCP4.5, (c) RCP6.0 and (d) RCP8.5. The red dots/bars denote warm-and-humid days. The solid and dashed blue lines denote the climatological (1966-2005) start and end of the warm-and-humid season respectively.